TiO 2 /Zeolite Bifunctional (Photo)Catalysts for a Selective Conversion of Methanol to Dimethoxymethane: On the Role of Brønsted Acidity

Kawthar Ftouni, Louwanda Lakiss, Sébastien Thomas, Marco Daturi, Christian Fernandez, Philippe Bazin, Jaafar El Fallah, Mohamad El-Roz

TiO_2/Zeolite Bifunctional (Photo)Catalysts For a Selective Conversion of Methanol to Dimethoxymethane: On The Role of Brønsted Acidity

*Kawthar Ftouni,[†] Louwanda Lakiss,[†] Sebastien Thomas,[§] Marco Daturi,[†] Christian Fernandez,[†] Philippe Bazin,[†] Jaafar El Fallah,[†] Mohamad El-Roz [†]**

† Normandie Univ, Ensicaen, Unicaen, CNRS, Laboratoire Catalyse et Spectrochimie, 14000 Caen, France.

§ Université de Strasbourg, Institut de chimie et procédés pour l'énergie, l'environnement et la santé, 67087 Strasbourg, France

Abstract

In the present work, we report the first example of one-step selective methanol photooxidation to dimethoxymethane (DMM) at room temperature over TiO_2/zeolite bifunctional catalysts. The effects of the porosity, basicity/acidity of the zeolites on the selectivity of the reaction are discussed. The role of TiO_2 active sites and zeolitic Brønsted acid sites on the DMM production is reported. As the photocatalytic reaction occurs at room temperature, the influence of the reaction temperature is also investigated to extrapolate the results to thermal catalysis. This study demonstrates a clear synergetic effect of the zeolites on the selectivity of the reaction. They can display an important impact on the selectivity of the photocatalytic reaction even at a low temperature (e.g. room temperature). Based on the obtained results, the reaction mechanism of methanol conversion to DMM is elucidated.

Introduction

Designing new catalysts for selective methanol oxidation to valuable products such as dimethoxymethane (DMM),[1] methyl formate (MF),[2] formaldehyde (FA),[3] or dimethyl ether (DME)[4] is of a high importance. Indeed, the demand for DMM has grown steadily in the last years owing to the remarkable growth of pharmaceutical industries. Due to its high chemical stability and low toxicity, DMM in fact is extensively used in cosmetic manufactures, as diesel fuel additive, as chemical intermediate and as an excellent solvent in perfume industries.[5,6,7]

At an industrial scale, DMM is produced from a homogeneous reaction of formaldehyde with methanol over acidic catalysts.[8] However, this approach is very expensive. It involves a high reaction temperature and often causes equipment corrosion due to the presence of acidic catalysts. Therefore, a one-step selective oxidation of methanol to DMM is strongly recommended for economic and environmental reasons.

The selective oxidation of methanol to DMM may involve two steps: (1) oxidation of methanol to formaldehyde on redox sites and (2) condensation of formaldehyde produced with additional methanol to DMM on acidic sites.[9] Thus, bifunctional catalysts with redox and acidic characters are required for the reaction. In addition, the relative strengths of surface acidity and redox ability of a catalyst may be important in determining the reaction pathways as well as the selectivity.

Several catalysts such as supported Ruthenium[10] and Rhenium oxides,[11] $SbRe_2O_6$,[12] heteropoly acids,[13] Cu-ZSM-5,[14] V_2O_5/TiO_2,[15] and VOx/TS-1,[16] etc. have been used for this procedure. Besides, the required reaction temperature is between 423 to more than 593 K.

Recently, we have reported that VO_x/Beta zeolite can promote the DMM formation by a photocatalytic conversion of methanol at room temperature.[17] However, the reaction was not selective and the DMM formation was related to the photocatalyst and the role of the support was indefinite. Contrariwise to VO_x based photocatalyst, no DMM was detected as a product of methanol photooxidation using pure titanium oxide as photocatalyst.

Despite the wide use of supports for enhancing photocatalytic activities,[18,19] the influence of these supports on the selectivity of the photocatalytic reaction is rarely assumed. This is mainly related to

the fact that photocatalytic reactions mainly occur at near room temperature and under mild reaction conditions. In such conditions, only the photoactive sites are involved in the reaction.

We report herein the first example of a one-step DMM production from methanol photooxidation at room temperature over bifunctional TiO_2/zeolite catalysts. We demonstrate that the selectivity of the photocatalytic reaction can be tuned and controlled by adjusting the reaction conditions and zeolite properties. In order to study the effect of zeolite type (supposed as support) on the selectivity of the reaction, several materials have been selected based on their acidity/basicity and porosity. The methanol photooxidations over TiO_2 combined with the different materials (porous, non-porous, acidic, basic) were performed under similar conditions. The reaction mechanism of methanol conversion to DMM is then proposed.

Experimental part

TiO_2-P25 (TiO_2) photocatalyst (Evonik Degussa) was used as received without any additional treatment. The different samples are prepared by solid state dispersion of 10 ± 2 wt.% TiO_2 with the different materials. SiO_2 (Ultrasil 7000, Evonik), commercial LZY-54 (Na^+-form, UOP, Si/Al = 2.3), LZY-64 (NH_4^+-form, UOP, Si/Al = 2.3), a micron-sized ZSM-5(M) (Si/Al = 23, Clariant), and a nanometer-sized ZSM-5(N) (Si/Al = 47, Clariant) are used as supplied without any treatment.

Beta (Si/Al = 15), and purely siliceous MFI (Silicalite) zeolites were synthesized following the protocol reported in the references [20,21], respectively. γ-alumina was prepared by heating a pseudoboehmite (Catapal B from Sasol) at 823 K for 5 h with a heating rate of 2 K/min under atmospheric condition. The acidic properties of the catalysts are determined by IR spectroscopy of adsorbed pyridine using a conventional glass cell. Infrared spectra are recorded on a Nicolet Magna 550-FT-IR spectrometer at 2 cm^{-1} optical resolution. Prior to the measurements, the catalysts are pressed into self-supporting discs (diameter: 1.6 cm, 20 mg cm^2) and pretreated *in-situ* under vacuum (10^{-6} Torr) at 823 K (2 K /min) for 5 h. Pyridine is adsorbed at 373 K. After establishing a pressure of 1 Torr at equilibrium, the cell is evacuated at 523 K to remove the physisorbed species. The amount of pyridine adsorbed on the Brønsted (1545 cm^{-1}) and Lewis (1454 cm^{-1}) sites is determined by integrating their respective band areas using the following extinction coefficients: $\varepsilon_{(B)1545}$ = 1.35 and $\varepsilon_{(L)1454}$ = 1.5 $cm.mol^{-1}$ for Py, respectively.[22] For LZY-64-NH_4^+, the analysis was performed on two different samples: 1) LZY-64-NH_4^+ pretreated *in-situ* under vacuum (10^{-6} Torr) at 823 K (2 K /min) for 5 h, 2) LZY-64(H) which was calcined under air at 823 K (2 K /min) for 5 h and then pretreated *in-situ* under vacuum (10^{-6} Torr) at 823 K (2 K /min) for 5 h. The values for LZY-64(H) are reported between brackets in Table 1.

The textural and the acidic properties of the different materials used in this work are summarized in the table 1.

Table 1. Textural and acidic properties of the different materials used in this work.

Sample	SiO_2	Silicalite	LZY-54 (Na)	ZSM-5 (M)	ZSM-5 (N)	LZY-64 (H)	Beta (H)	γ-alumina
Si/Al lattice	/	/	2.3	23	47	2.3	15	/
BET ($m^2.g^{-1}$)[(a)]	400	420	906	377	488	754	635	254
V_{mic} ($cm^3.g^{-1}$)[(b)]	/	0.17	0.34	0.18	0.17	0.34	0.25	/
S_{ext}($m^2.g^{-1}$) [(c)]	/	125	60	9	75	60	164	243
B_{Py} (μmol.g^{-1}) [(d)]	/	/	/	617	224	1320 (220)[(f)]	274	/
L_{Py} (μmol.g^{-1}) [(e)]	/	/	/	91	67	45 (690)[(f)]	163	370
Particle size (nm)[(g)]	100	100	800	600	25 (100)	500	20 (100)	20 (600)

(a) Specific surface area measured by BET; (b) microporous volume and (c) External surface area calculated using the t-plot method; (d) Brönsted and (e) Lewis acidity; (f) values calculated after the calcination of the ammonium form under air. (g) The particle sizes are determined according to SEM micrographs. The values between brackets correspond to the size of the aggregates.

The catalysts were then pressed into self-supported wafers (Ø = 16 mm, m~10 mg/cm^2) with a thickness of about 65 ± 2 μm as measured by scanning electron microscopy (SEM, Tescan MIRA FEG).

The outlet gas phase evolution was followed by both IR spectroscopy and mass spectrometry. FTIR spectra of the outlet gas phase and of the surface were collected with a Nicolet 5700 FT-IR spectrometer (64 scans/spectrum) equipped with a MCT detector. The *operando* system was connected to a flow set-up.[23] Gases were introduced into the lines by mass flow controllers. The system allows the two gas mixtures, so-called "activation" and "reaction" flows, to be prepared and sent independently to the reactor cell. The "sandwich" type reactor-cell used in this study is described in reference [24]. It was made of a stainless-steel cylinder that carries a toroidal sample holder in its center, where the catalyst self-supporting wafer was placed. Tightness was obtained by O-rings, and the dead volume (typically defined as the residual space between each sample face and the windows) was reduced to about 0.4 mL by filling the empty space with KBr windows placed on each side of

the sample holder. The surface analysis was made possible without the superposition of the gas phase signal and fluid dynamics. Gases were introduced to the sample by 1/8-inch OD pipe and collected on the opposite side of the sample holder. For this specific photocatalytic oxidation study, UV irradiation was carried out with a polychromatic light of Xe-Hg lamps (LC8 spot light Hamamatsu, L10852, 200 W). It has been performed by using a UV-light guide (A10014-50-0110) mounted at the entrance of a modified *operando* IR cell to establish a homogeneous and similar irradiation on the different photocatalysts pellet surfaces. More details can be found in references [24] and [25]. In order to avoid any possible heating of the samples due to the IR emission of the lamp, a "Block infrared light" filter (Hamamatsu A9616-10) with a transmittance wavelength from 300 to 400 nm have been used in this work. The lamp irradiance was measured using ILT950 spectrilight spectroradiometer from International Light Technologies. All samples have been activated under dry synthetic air (*in situ*) at relatively low temperature (423 K) for 2h in order to preserve their original properties. The activation process was enough for removing the majority of adsorbed water.

The employed configuration allowed a low partial pressure of methanol to be achieved using a saturator at controlled temperature. The gas mixture composition was fixed then at 0.12 vol. % methanol and 20 vol. % O_2 in Ar and the total flow was adjusted to 20 cm^3/min. The analysis of the outlet gases was performed by means of a Pfeiffer Omnistar mass spectrometer. Likewise, FT-IR spectra of the gas phase were collected using a gas microcell. The selectivity and the conversion were calculated using the calibration curves for the different products involved in the reaction. In this work, the light intensity of the lamp was adjusted in order to obtain a similar conversion around 35% (for preventing the effect of the mass transfer on the selectivity). The IR gas cell used in this work for analysing the reaction gas phase was previously calibrated with the different standard products expected from methanol photooxidation. This allows the determination of the concentration of the products in the gas phase. More experimental details are given in references (25-26). It should be noted that no deactivation of the catalyst is observed under the reaction conditions used in this study. This agrees with our previous observation on methanol photooxidation on TiO_2 based photocatalyst at relatively low temperature.[24] Each experiment was repeated at least twice and the average values are reported (error estimated lower than 10% on the different experiments).

Results and discussion

FTIR spectroscopy and mass spectrometry, connected on line with the *operando* IR reactor for analyzing the gas phase, complementarily allows the identification of the reaction products and the determination of reaction conversion and selectivity, calculated at the steady state (after stabilization for 2h). The conversion of methanol is calculated by using the ν(OC) vibrational band of methanol at 1034 cm^{-1}.[26] As already mentioned in the experimental part, the conversions were maintained between 30 and 40% (by adjusting the lamp intensity) in order to reduce the effect of mass transfer

on the selectivity. The IR spectra of the reaction gas phase, at the steady state, during methanol photooxidation on supported TiO_2 photocatalysts are assembled in Figure 1. The following products have been identified: Formaldehyde (FA), methylformate (MF), dimethyl ether (DME), dimethoxymethane (DMM), and carbon dioxide. A calibration (on IR and MS) of these products have been previously performed using standard products in order to calculate their selectivity. The selectivity of CO_2 was determined by using the $\nu(CO_2)$ vibration band at 2300-2200 cm^{-1} (Figure 1). A deconvolution of the IR spectra in the 1650-1850 cm^{-1} vibration region was necessary for determining the concentration of MF and FA using $\nu(C=O)$ vibration bands at 1754 cm^{-1} and 1748 cm^{-1}, respectively. A deconvolution of the IR spectra in the 1650-1850 cm^{-1} region was necessary for determining the concentration of MF and FA using $\nu(C=O)$ vibration bands at 1754 cm^{-1} and 1748 cm^{-1}, respectively. The overlapping of these bands makes the precise determination of the formaldehyde concentration a challenge. Therefore, the IR spectrum of the reaction gas phase at the steady state was first subtracted from the original spectrum of a pure MF standard (250 ppm/Ar) using Omnic software. A subtraction factor was applied until the disappearance of the characteristic IR bands of MF (see Figure 1-B). Using this factor, the MF formate concentration was then determined as a multiplicity of this factor (f) and the MF concentration (f x 250 ppm). The result was compared to that obtained from the mass spectrometer using the signal of MF at m/z = 60. Contrarily to the MS signals of FA, there is no contribution of other products at m/z = 60. The values obtained were in agreement with those determined by IR for MF and the concentration of FA was then determined on the deconvoluted spectrum using the intensity of the band at 1748 cm^{-1} (after MF subtraction). For DMM, the $\nu(OC)$ vibration band at 1148 cm^{-1} and the MS signal at m/z = 75 have been used for calculating the selectivity. The so called “other compounds” added to some results represent minor species below the detection limits (e.g. formic acid or dimethyl ether in some cases) and complete the materials balance. It also accounts for the experimental error.

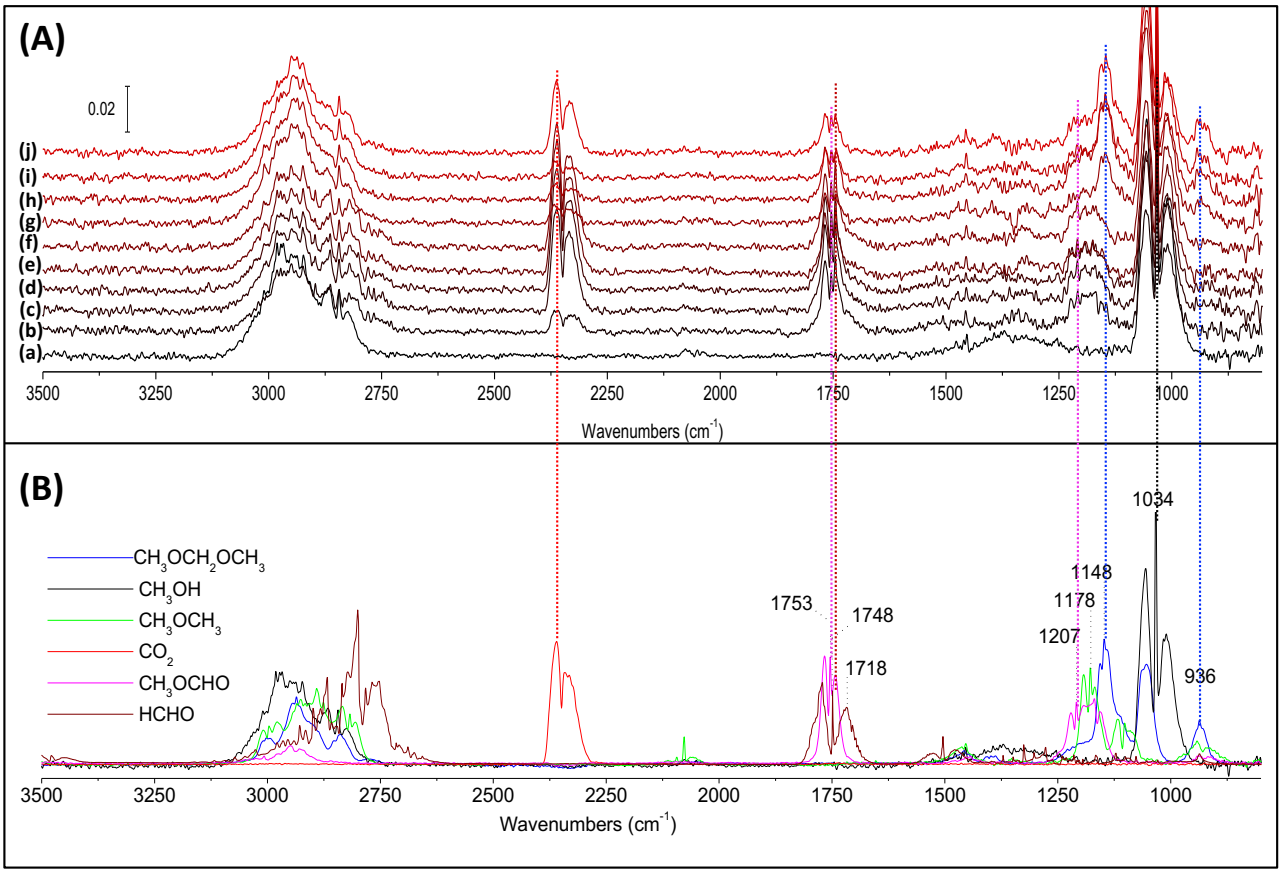

Figure 1/ (A) IR spectra of gas phase reaction (at steady state) during methanol photooxidation (at room temperature) over TiO_2 /oxides: (a) corresponds to the IR spectrum of methanol; (b) self-supported TiO_2; (c) SiO_2 (used as reference); (d) Silicalite; (e) LZY-54(Na-form); (f) γ-Al_2O_3; (g) LZY-64(H-form); (h) ZSM-5 (N); (i) ZSM-5 (M); and (j) Beta(H). (B) IR spectra of methanol and possible products collected by sending them in Ar flow to the IR cell (except FA IR spectrum which is used from the data base of Omnic software). Reaction conditions: flow = 20 cm^3/min; [methanol] = 1200 ppm; 20% O_2/Ar; T = 298 K; TiO_2/support = 10 ± 2 wt./wt. %; m_{cat} = 20 ± 1 mg. Dotted lines correspond to the position of the characteristic IR bands of the identified products.

The effect of the zeolites and other supports (SiO_2 and Al_2O_3) on the selectivity of methanol photooxidation on TiO_2 is illustrated in Figure 2. Indeed, the different types of zeolites and oxides used as supports in this work can be classified as follows: i) neutral support (SiO_2); ii) neutral zeolite (purely siliceous MFI; silicalite); iii) zeolite with Lewis base sites (LZY-54); iv) support with only Lewis acid sites (γ-Al_2O_3); and v) zeolites with Lewis and Brønsted acid sites (LZY-64(H), ZSM-5(M), ZSM-5(N) and Beta(H)). LZY-64(NH_4^+) is the ammonium form of LZY-54(Na) that will be directly transformed to acidic form LZY-64(H) after *in situ* calcination in the IR cell. For ZSM-5(M) and ZSM-5(N) supports, the only differences are their crystal size and Si/Al ratios (23 and 47, respectively). For comparison, self-supported (S.S.) TiO_2 wafer is also used as a reference. As shown in Figure 2, porosity has no impact on the selectivity; since silica and purely siliceous microporous

MFI zeolite (silicalite) showed similar results as the self-supported TiO_2. γ-alumina also shows similar results demonstrating that Lewis acidity has also no significant impact on the selectivity. Only zeolites with Brønsted acid sites have an important impact on the selectivity of the reaction. It should be noted, that there is no activity observed without TiO_2 and/or in the dark.

Based on our previous work,[27] the thermo- and/or photo-dissociation of the methanol is the first step of methanol photooxidation reaction on TiO_2. After that, the first oxidation of the adsorbed methoxy species leads to the formation of FA. At a low methanol concentration (or conversion), FA desorption is promoted and this latter is detected as a main product of the reaction. Otherwise, a second oxidation of the adsorbed FA occurs and formal/formate species are then formed. These species are in a scrambling movement on the surface.[26,27] When these species come across a hole, an additional oxidation is promoted and yields to CO_2. MF is the product of the crosslinking of the formyl species with adsorbed methoxy on an adjacent site. This product is promoted with the increase of methoxy concentration on TiO_2 surface. Indeed, the selectivity to MF can be tuned by adjusting the reaction conditions (e.g. methanol conversion or concentration) without need to change the photocatalyst. However, DMM is exclusively formed with a high selectivity over bifunctional TiO_2/zeolite catalysts with acid sites. As there is no formation of DMM on TiO_2/Al_2O_3, the possible role of the Lewis site in the DMM formation can be eliminated. Consequently, the presence of the Brønsted acid sites is at the origin of the DMM formation which is in agreement with the previous results obtained on the thermal oxidation of methanol.[28]

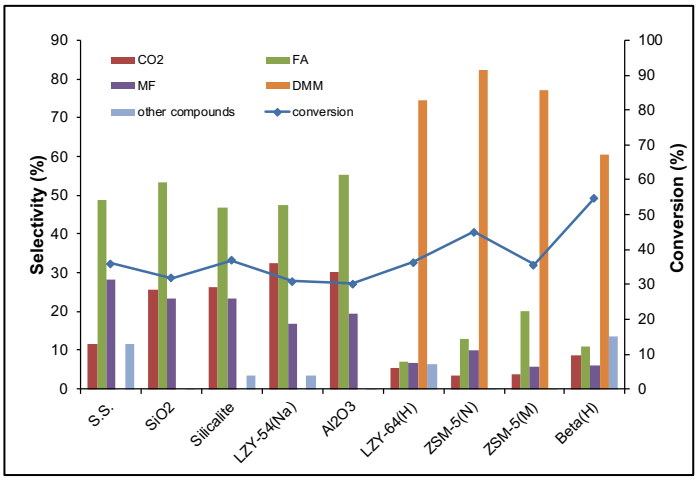

Figure 2/ Conversion and selectivity of methanol photooxidation over supported TiO_2-P25 (prepared by solid state dispersion); (S.S.) corresponds to the self-supported TiO_2. N.B. Irradiation adjusted in order to obtain a similar conversion (35 ± 5%). Reaction conditions: flow = 20 cm^3/min; [methanol] = 1200 ppm; 20% O_2/Ar; T = 298 K; m_{cat} = 20 ± 1 mg; TiO_2/support = 10 ± 2 wt./wt. %.

Operando FTIR setup used in this work allows a time-resolve, simultaneous quantitative analysis of the photocatalyst surface species and the gas phase products.[24] The low transparency of some zeolites toward IR in the 2500-1000 cm^{-1} vibration region makes the analysis of the IR data of the surface

complex. Nevertheless, the IR results of the surface of some catalysts which demonstrate different selectivity were successfully treated and reported in Figure 3. Indeed, the low content of TiO_2 (10 wt.%) in addition to the high adsorption capacity of zeolites make difficult to distinguish between the adsorbed species on TiO_2 active sites and the products adsorbed on zeolites/supports. However, the comparison of the recorded IR data of the different samples reveals some interesting information. New IR bands appear after the first minutes of irradiation. Two carbonyl vibration bands are observed in the case of TiO_2/SiO_2 and TiO_2/silicalite at 1736 and 1715 cm^{-1}, whereas only one band at 1715 cm^{-1} is observed in the case of TiO_2/Beta. The band at 1715 cm^{-1} is assigned to the stretching vibration of the carbonyl of adsorbed formaldehyde[29] while the band at 1736 cm^{-1} is assigned to the stretching vibration of the carbonyl of adsorbed methylformate. Due to the different affinity of SiO_2 and silicalite vs. reaction products, the relative concentration of the adsorbed products is not the only factor affecting the intensity of the corresponding IR bands. However, the band intensity at 1715 cm^{-1} observed in TiO_2/Beta is 10 times higher than that observed for TiO_2/SiO_2 and TiO_2/silicalite. The bands at 1500-1300 cm^{-1} are mainly assigned to the adsorbed formaldehyde and related species. The decrease of the band at 1630 cm^{-1} in the case of TiO_2/Beta is attributed to the desorption of residual water on the highly hydrophilic Beta zeolite.

As reported in Table 1, the difference in the surface area and microporous volumes between silicalite and Beta zeolites is not very significant. Basing on the gas phase data, the amount of produced FA and MF is more important on TiO_2/silicalite than on TiO_2/Beta. Therefore, in the case of Beta zeolite, the formaldehyde is probably an intermediate more than a final product. The low amount of adsorbed MF on Beta is mainly due to the low amount of this product. This can be explained by the low oxidation of FA into formyl as we can observe from the low IR band intensity of these species (broad band centered at ≈1570 cm^{-1}) in the case of TiO_2/Beta in respect to TiO_2/SiO_2 and TiO_2/Silicalite. These results agree with the low amounts of CO_2 and MF obtained on TiO_2/Beta(H) catalyst where formyl species are the common intermediates of these products.[27,30,31]

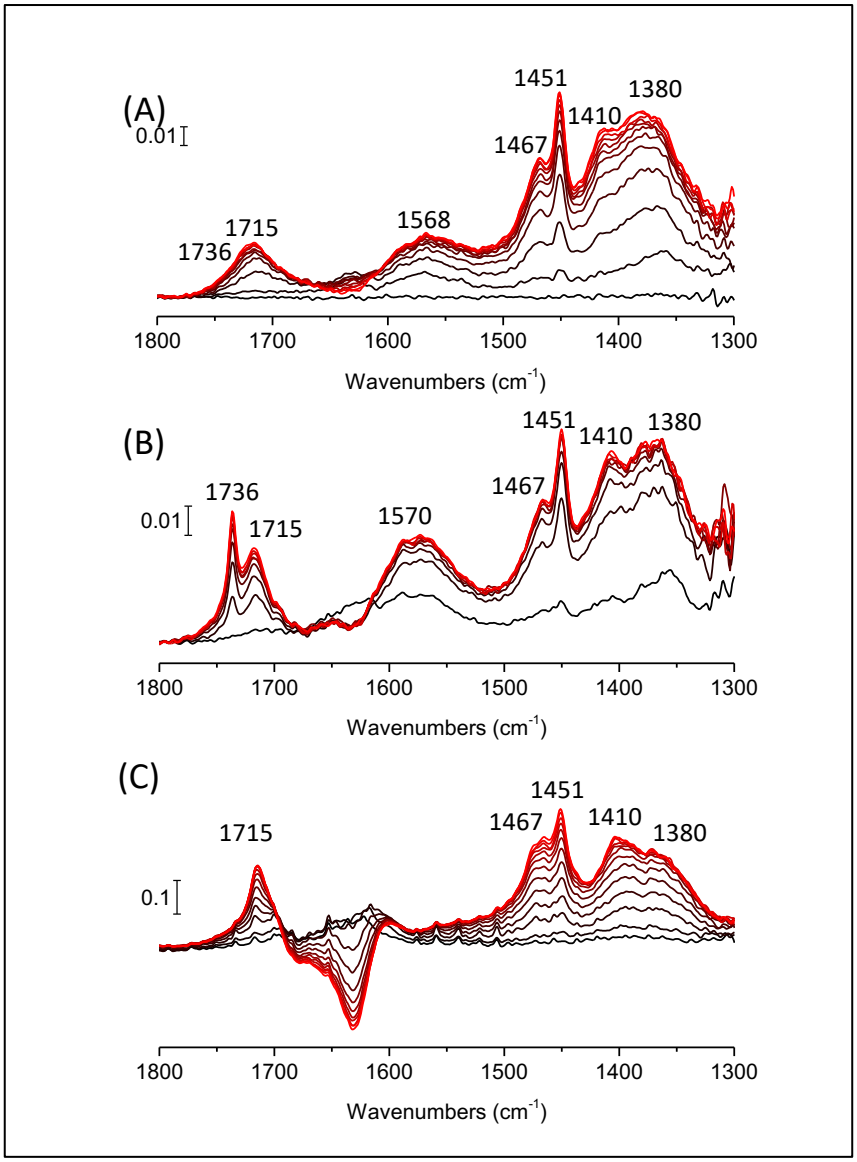

Figure 3/ IR spectra of the adsorbed surface species on TiO_2/SiO_2 (A), TiO_2/Silicalite (B) and TiO_2/Beta(H) (C) during the first minutes of irradiation (2 min/spectrum). The spectra were subtracted from the IR spectrum of the sample before irradiation. Reaction conditions: flow = 20 cm^3/min; [methanol] = 1200 ppm; 20% O_2/Ar; T = 298 K; m_{cat} = 20 ± 1 mg; TiO_2/support = 10 ± 2 wt./wt. %.

In order to shed more light on the role of the Brønsted acid sites in DMM formation at room temperature, methanol photooxidation have been performed, under similar conditions, on TiO_2 mixed with the same zeolite type under different forms: LZY-54(Na), LZY-64(NH_4^+), and LZY-64(H). The results are presented in Figure 4. As it is already observed, there is no formation of DMM on LZY-54(Na) while DMM is produced with a high selectivity (≈ 90 ± 5 %) on LZY-64(H). Contrariwise to TiO_2/LZY-54(Na), TiO_2/LZY-64(NH_4^+) showed a selectivity of about 30% toward DMM. This indicates the presence of Brønsted acid sites in the ammonium form. These sites might be generated during the reaction due to NH_3 oxidation into NO_x product releasing the Brønsted acid sites.

Unfortunately, it was difficult to confirm this information by IR analysis of the surface during the reaction due to the saturation on bands intensity in the region of ammonium vibrations and the low transparency of these samples in IR.

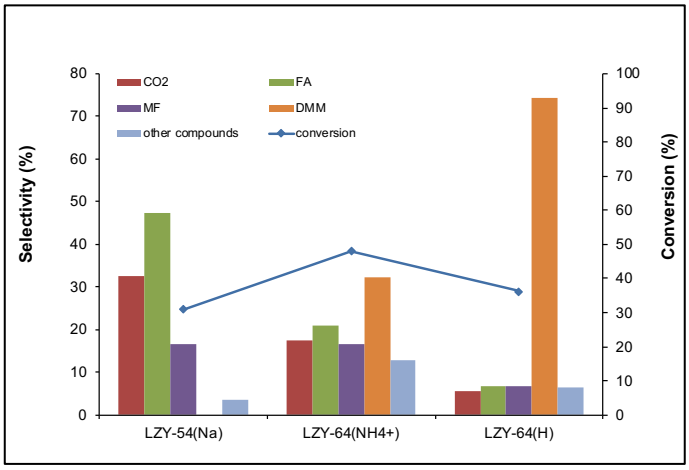

Figure 4/ selectivity of methanol photooxidation on TiO_2-P25 mixed with zeolite Y in different forms: sodium form (LZY-54(Na^+); ammonium form (LZY-64(NH_4^+)); and acidic form (LZY-64(H)). LZY-64(H) obtained after the calcination of LZY-64(NH_4^+) at 550°C under vacuum. The conversion is also reported and maintained at around 30 ± 5%.

An additional experiment of methanol photooxidation was performed for clarifying the possibility of the existence of Brønsted acid sites in the inactivated LZY-64(NH_4^+). A UV activation of TiO_2/LZY-64(NH_4^+) was performed, before the reaction, for 3 hours under synthetic air and at room temperature. The evolution of the methanol, methylformate and dimethoxymethane in the gas phase was followed by IR and mass spectrometry. For comparison, the same experiment was realized on the same sample without any previous activation. The normalized results are presented in Figure 5. Figure 5-A represents the evolution of methanol in the gas phase before and after sending methanol through the reactor. The adsorption equilibrium of methanol is reached after 40 and 50 min (the minimum time required to detect methanol in the gas phase) on the non-activated and activated TiO_2/LZY-64(NH_4^+) samples, respectively. This difference in the equilibrium delay may be related to the increase of the adsorption capacity of TiO_2/LZY-64(NH_4^+) toward methanol after UV activation. Indeed, the oxidation of ammonium species generates Brønsted acid sites which increases the adsorption capacity. The evolution of the MF and DMM is reported in Figure 5-B. MF is detected in the first minutes of the reaction. This is in agreement with the fact that MF is selectively formed on TiO_2 surface and means that the affinity of the support toward MF is relatively low in respect to that of methanol and/or other products (e.g FA). However, an induction time of 100 minutes is observed for DMM on the non-activated sample. This delay is reduced to 40 minutes on the activated one. The experiment was repeated twice and reproducible results are obtained. These results demonstrate without any doubt the generation of new Brønsted acid sites on TiO_2/LZY-64(NH_4^+) during the photocatalytic reaction. In other words, a partial photocatalytic activation of TiO_2/LZY-64(NH_4^+) is

possible and explains the formation of DMM on non-activated TiO_2/LZY-64(NH_4^+). Therefore, the generated oxidant species (Ozone, HO radical, etc.) can have a relatively long lifetime in the gas phase and can leave the photocatalyst surface for promoting oxidation reaction of adsorbed NH_3 on a Brønsted site (H^+) in the zeolite surface/porosity.

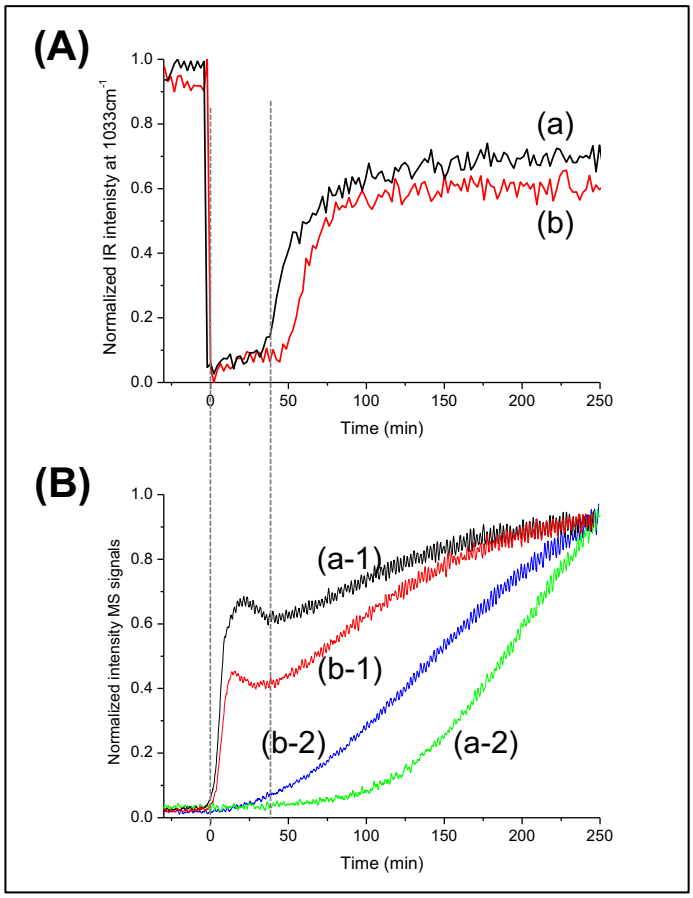

Figure 5/ (A) Evolution of the characteristic IR band of methanol at 1033 cm^{-1}, in the gas phase during methanol photooxidation on TiO_2-P25/LZY-64(NH_4^+) (a) without activation and (b) after photoactivation by UV irradiation (lamp Hg-Xe; 200W). (B) Corresponding evolution of the MS intensities of (1) m/z = 60 (characteristic of MF) and (2) m/z = 75 (characteristic of DMM) during methanol photooxidation on the samples (a) and (b). t = 0 min corresponds to the time that methanol pass through the reaction flow. Reaction conditions: flow = 20 cm^3/min; [methanol] = 1200 ppm; 20%O_2/Ar; T = 298 K; mcat = 20 ± 1 mg; TiO_2/support ratio = 10 ± 2 wt./wt. %.

The role of the heterogeneous bifunctional catalysts interface on the selectivity of the primary alcohol oxidation over metal/oxide catalysts was recently demonstrated.[32,33] In our case, there are two possible ways for the formation of DMM over supported TiO_2 on acidic zeolites: i) DMM is formed at the TiO_2/zeolite interface. This means that neighbor TiO_2 active sites and Brønsted acid sites on the external zeolite surface are required; or ii) DMM is formed in two consecutive steps: first, by the oxidation of methanol to FA on TiO_2. Then, the produced FA is adsorbed/protonated on the Brønsted acid sites where it will be followed by condensation reactions with methanol.

In order to elucidate these two hypotheses, methanol photooxidation was performed on two separated and superposed pellets, self-supported TiO_2 and Beta(H) (called TiO_2+Beta), respectively. The two pellets are placed on the same samples holder in the *operando* cell. Therefore, the physical contact between the photocatalyst and the zeolite support is negligible compared to the mechanical mixture. The result is presented in Figure 6. For comparison, methanol photooxidation under similar conditions has been performed over TiO_2/Beta(H) (mechanical mixture) and TiO_2 supported on the as synthetized Beta (TiO_2/Beta(a.s.)) sample (the organic template is not removed by calcination). Contrary to the TiO_2/LZY-64(NH_4^+) sample, there is no formation of DMM observed using the as synthesized Beta zeolite. Therefore, we can discard the existence and creation of Brønsted acid sites during the photocatalytic reaction on this catalyst. For TiO_2+Beta sample, a similar selectivity as for TiO_2/Beta(H) prepared by solid state dispersion is observed. Consequently, the interface TiO_2/zeolite has no consequence in the formation of DMM. This assumption means that the DMM formation is promoted even at room temperature on Brønsted acid sites in the presence of a stoichiometric amount of formaldehyde and methanol. Despite the important role of the Brønsted acid sites in the formation of DMM, the role of the Lewis sites cannot be excluded. A synergetic effect of the Brønsted/Lewis acid sites could be observed.[34,35]

As we mentioned above, the methanol conversion was maintained constant for all experiments. This justifies why the amount of the DMM formed and the Brønsted acidity of the samples are not dependent (Table 1). Other factors as the internal diffusion and/or the acidity strength might have an impact on the reaction rates but not on the selectivity. A separated study using steady state isotopic transient kinetic analysis (SSITKA) is in progress to determine the reaction parameters (e.g. diffusion constant, etc.) basing on the results obtained in this work.

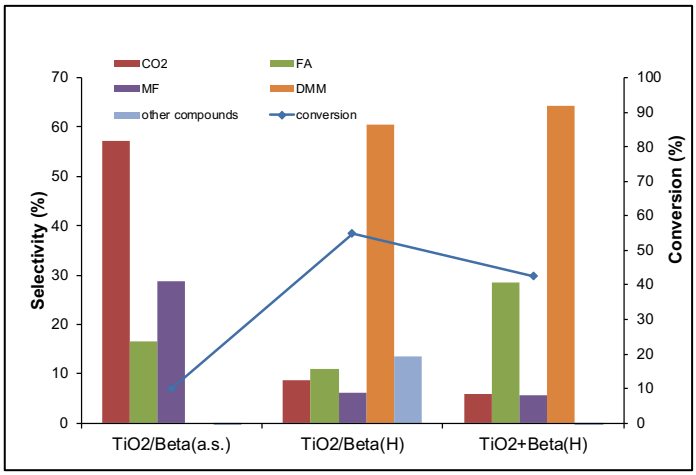

Figure 6/ Methanol photooxidation selectivity and conversion on TiO_2-P25 mixed with as synthesized Beta zeolite (TiO_2/Beta(a.s.)), with calcined Beta zeolite (TiO_2/Beta (H)). TiO_2+Beta corresponds to the sample where TiO_2 and Beta zeolite are prepared in two separated and superposed pellets (negligible physical contact between the two pellets (diameters = 16 mm)). Reaction conditions: flow

= 20 cm^3/min; [methanol] = 1200 ppm; 20% O_2/Ar; T = 298 K; m_{cat} = 20 ±1 mg; for TiO_2+Beta: m_{TiO2} = 10 mg, $m_{Beta(H)}$ = 10 mg.

The effect of the temperature on the reaction selectivity has been investigated on TiO_2/LZY-54(Na) and (B) TiO_2/LZY-64(H) samples. The results are exposed in Figure 7. The increase of the temperature promotes the total oxidation versus the partial oxidation on TiO_2/LZY-54(Na). This result agrees with the previous result obtained on self-supported TiO_2 photocatalyst.[24] However, the increase of the temperature for TiO_2/LZY64(H) has a dramatic effect on the formation of DMM, nevertheless, the formation of DME is promoted. As no DME is detected in the case of TiO_2/LZY-54(Na), the acidic sites of the LZY64(H) are at the origin of the dehydration of methanol at a relatively high temperature. The dramatic decrease of DMM selectivity is not related to the total oxidation as we can understand from the low selectivity to CO_2. Therefore, it is mainly due to the weak adsorption of formaldehyde when increasing the temperature. These results demonstrate that FA is an intermediate product of methanol photooxidation when a catalyst/support with Brønsted acidity is used and it is weakly adsorbed on the surface. The presence of the Brønsted active sites promotes the adsorption of formaldehyde, decreases its contact time with the photocatalyst surface, therefore its oxidation on the photocatalyst surface, and lead to the formation of DMM.
These results can be extrapolated for the thermo-catalytic oxidation of methanol and not only for the photocatalytic oxidation. In the thermal formation of DMM, a high temperature is required for the formation of FA on oxidant sites, while DMM can be formed with a high selectivity on the Brønsted acid sites at nearly room temperature.

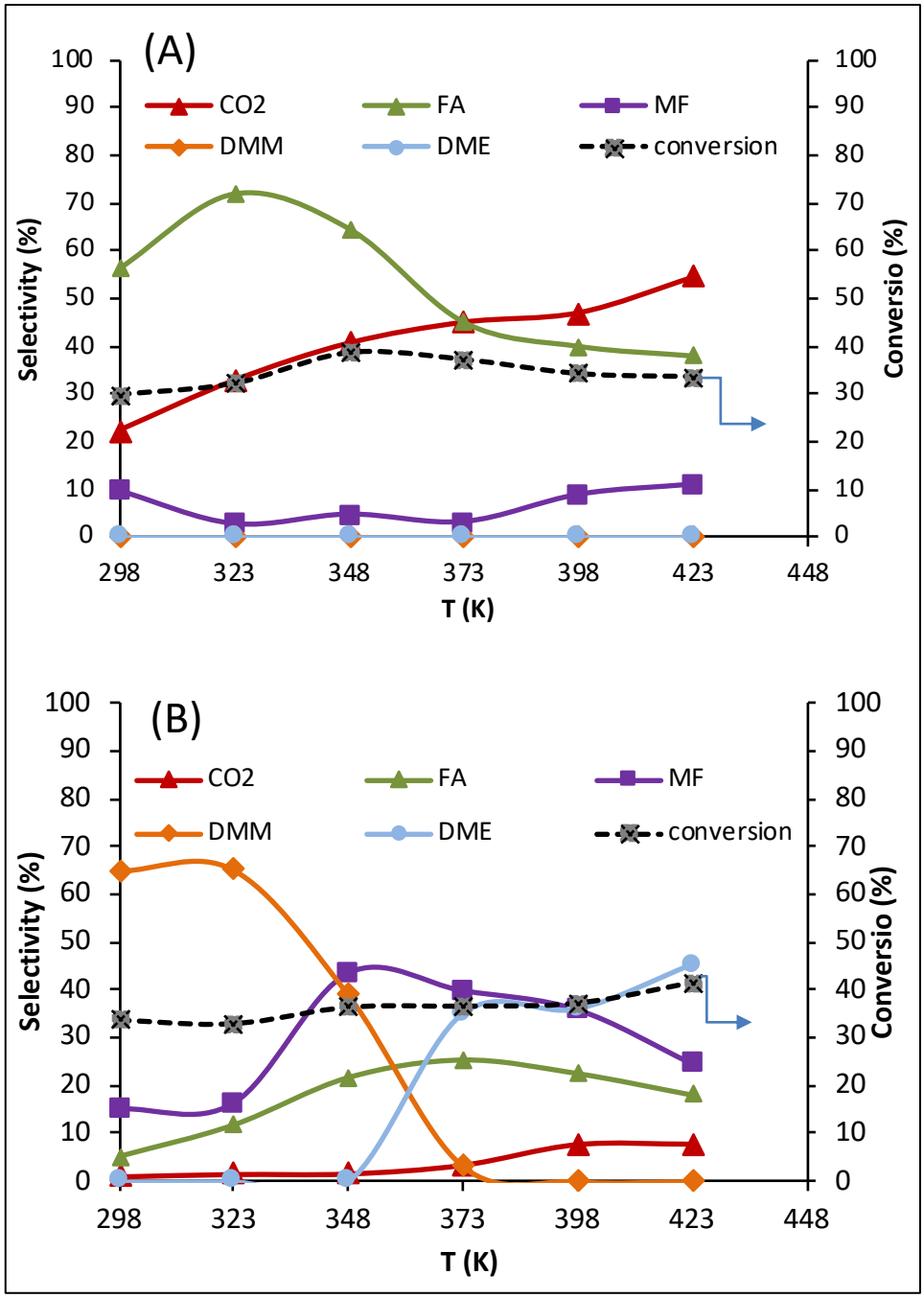

Figure 7/ Evolution of the selectivity of the methanol photooxidation reaction over (A) TiO_2/LZY-54(Na) and (B) TiO_2/LZY-64(H) versus the temperature. The conversion was maintained at 30 ± 5% by adjusting the lamp intensity. Uncertainty ≈5%.

Based on the previous results, the mechanism of methanol photooxidation to dimethoxymethane can be proposed as follows: TiO_2 promotes the photooxidation of methanol to FA while zeolite promotes the adsorption and the protonation of methanol and/or formaldehyde on the Brønsted acid sites. A nucleophilic attack followed by a condensation reaction with methanol occurs and DMM is then formed (Scheme 1). This mechanism is in agreement with that reported recently in the literature.[30,36]

(1) $CH_3OH_{(g)} + HO_{(s)} \leftrightarrows CH_3O_{(a)} + H_2O_{(g)}$ (cat, Δ)

(2) $CH_3OH_{(g)} + ½\ O_{2(g)} \rightarrow CH_3O_{(a)} + HO_{(s)}$ (cat, hν)

(3) $CH_3O_{(a)} + ½\ O_{2(g)} \rightarrow CH_2O_{(a)} + HO_{(s)}$ (cat, hν)

(4a) $CH_3O_{(a)} + CH_2O_{(a)} + (H^+, {}^-O=)_{(s)} \rightarrow (CH_3OCH_2OH^+, {}^-O=)_{(s)}$ (cat, Δ)

(4b) $CH_3OH_{(g)} + (CH_3OCH_2OH^+, {}^-O=)_{(s)} \rightarrow CH_3OCH_2OCH_3 + (H^+, {}^-O=)_{(s)} + HO_{(s)}$ (cat, Δ)

(5) $2CH_3O_{(a)} \rightarrow CH_3OCH_{3(g)} + O_{(s)}$ (cat, Δ)

(6) $CH_2O_{(a)} + HO_{(s)} \rightarrow CHO_{(a)} + H_2O_{(g)}$ (cat, hν)

(7) $CH_3O_{(a)} + CHO_{(a)} \rightarrow CH_3OCHO_{(g)}$ (cat, Δ)

(8) $CHO_{(a)} + ½\ O_{2(g)} \rightarrow CO_{(g)} + HO_{(s)}$ (cat, hν)

(9) $CHO_{(a)} + O_{2(g)} \rightarrow CO_{2(g)} + HO_{(s)}$ (cat, hν)

(10) $CH_2O_{(a)} + ½\ O_2 \rightarrow CH_2O_{(g)} + O_{(s)}$

(11) $2HO_{(s)} \rightarrow H_2O_{(g)} + ½\ O_{2(g)}$ (cat, hν)

(a) Adsorbed species
(s) surface species
$(H^+, {}^-O=)$ Brønsted site
(g) gas phase
cat= catalyst
(cat, hν): photocatalytic reaction
(cat, Δ) catalytic reaction at near RT

Scheme 1. Main steps of the photocatalytic methanol oxidation, at room temperature, to dimethoxymethane over TiO_2 supported on zeolite support with Brønsted/Lewis acid sites.

Despite that this work is intended to explain the selective methanol photooxidation, the obtained results can be extrapolated also to thermal catalysis. We can assume that a highly selective thermal oxidation of methanol to DMM is possible. However, the following conditions should be respected: a redox catalyst is necessary for selective methanol oxidation to FA (e.g. MoO_x, Ag-based catalyst, TiO_2 or V_2O_5). This reaction requires a relatively high temperature. In this step, a low methanol conversion is recommended to minimize the FA oxidation. The second step reaction can be held in the same reactor, however, a separate reactor (in series with the first one) containing a catalyst with Brønsted acid sites is recommended, and the condensation reaction is then promoted at near room temperature. As DMM is more stable than FA and MeOH, a loop configuration of the two reactors with recycling can be investigated in order to increase the yield of the reaction. In such a configuration, a heat exchanger between the two reactors is necessary to adjust the reaction temperature. Further work using different reactors configuration is required for demonstrating this hypothesis. In photocatalysis, there is no need to separate the two reactions as the reaction occurs at room temperature.

Conclusion

The mechanistic insights obtained by our investigations have shown that the selective oxidation of methanol to DMM involves first the oxidation of methanol to formaldehyde on redox sites and then the condensation of the produced formaldehyde with additional methanol to form DMM on acidic

sites. In thermal catalysis, the reaction temperature required for this procedure is between 423 and 593 K. In this work we have demonstrated the possibility to produce dimethoxymethane by selective methanol photooxidation at room temperature. The results demonstrate that the condensation step occurs near room temperature (305-310 K) and there is no role of the photocatalyst in this step. This latter is involved in partial methanol photooxidation to formaldehyde. The high selectivity of DMM is explained by a simultaneous adsorption of produced formaldehyde, on the Brønsted sites of the support, preventing its oxidation on the photocatalyst surface. This is in agreement with the low selectivity obtained on the Brønsted-free support and on the self-supported TiO_2. The increase of the temperature had a dramatic effect on dimethoxymethane formation. Therefore, we suggest that the best configuration of a setup for thermal selective methanol oxidation to dimethoxymethane would be obtained by using two connected batch reactors in a loop configuration: one with the redox catalyst at an optimized temperature, which promotes a selective partial oxidation of methanol to formaldehyde, while the second contains the catalyst with Brønsted acid sites (zeolite) at room temperature.

AUTHOR INFORMATION

Corresponding Author

*E-mail: mohamad.elroz@ensicaen.fr

Author Contributions

The manuscript was written through contributions of all authors. All authors have given approval to the final version of the manuscript.

ACKNOWLEDGMENT

M. El-Roz acknowledges the Labex project (EMC3) and The PHC-Tassili (18UMD983) for the financial support.

References

(1) Fu, Y.; Shen, J. Selective Oxidation of Methanol to Dimethoxymethane Under Mild

Conditions Over V_2O_5/TiO_2 With Enhanced Surface Acidity, *Chem. Commun.* **2007**, 2172-2174.

(2) Colmenares, J. C.; Lisowski, P.; Łomot, D.; Chernyayeva, O.; Lisovytskiy, D. Sonophotodeposition of Bimetallic Photocatalysts Pd-Au/ TiO_2: Application to Selective Oxidation of Methanol to Methyl Formate, *ChemSusChem* **2015**, *8*, 1676-1685.

(3) Hellier, P.; Wells, P. P.; Gianolio, D.; Bowker, M. VO_x/Fe_2O_3 Shell–Core Catalysts for the Selective Oxidation of Methanol to Formaldehyde, *Top Catal*, **2017**, 1-8.

(4) Rownaghi, A. A.; Rezaei, F.; Stante, M.; Hedlund, J. Selective Dehydration of Methanol to Dimethyl Ether on ZSM-5 Nanocrystals, *App. Cat. B: Environ.* **2012**, *119-120*, 56-61.

(5) Marrodań, L.; Royo, E.; Millera, Á.; Bilbao, R.; Alzueta, M. U. High Pressure Oxidation of Dimethoxymethane, *Energy Fuels* **2015**, *29*, 3507-3517.

(6) Zhu, R.; Wang, X.; Miao, H.; Huang, Z.; Gao, J.; Jiang, D. Performance and Emission Characteristics of Diesel Engines Fueled with Diesel-Dimethoxymethane (DMM) Blends, *Energy* Fuels **2009**, *23*, 286-293.

(7) Thavornprasert, K.; Capron, M.; Jalowiecki-Duhamel, L.; Dumeignil, F. One-pot 1,1-Dimethoxymethane Synthesis From Methanol: a Promising Pathway Over Bifunctional Catalysts, *Catal. Sci. Technol.*, **2016**, *6*, 958-970.

(8) Fuji, K.; Nakano, S.; Fujita, E. An Improved Method for Methoxymethylation of Alcohols under Mild Acidic Conditions, *Synthesis* **1975**, *4*, 276-277.

(9) Liu, H.; Iglesia, E. Selective One-Step Synthesis of Dimethoxymethane via Methanol or Dimethyl Ether Oxidation on $H_{3+n}V_nMo_{12-n}PO_{40}$ Keggin Structures, *J. Phys. Chem. B* **2003**, *107*, 10840-10847.

(10) Yuan, Y.; Iwasawa, Y. Performance and Characterization of Supported Rhenium Oxide Catalysts for Selective Oxidation of Methanol to Methylal, *J. Phys. Chem. B*, **2002**, *106*, 4441-4449.

(11) Liu, H.; Iglesia, E. Selective Oxidation of Methanol and Ethanol on Supported Ruthenium Oxide Clusters at Low Temperatures, *J. Phys. Chem. B*, **2005**, *109*, 2155.

(12) Yuan, Y.; Tsai, K.; Liu H.; Iwasawa, Y. Selective Methanol Conversion to Methylal on Re-Sb-O Crystalline Catalysts: Catalytic Properties and Structural Behavior *Top. Catal.*, **2003**, *22*, 9-15.

(13) Liu, H.; Bayat, N.; Iglesia, E. Site Titration with Organic Bases During Catalysis: Selectivity Modifier and Structural Probe in Methanol Oxidation on Keggin Clusters, *Angew. Chem., Int. Ed.,* **2003**, *42*, 5072-5075.

(14) Zhang, Y.; Drake, I. J.; Briggs, D. N.; Bell, A. T. Synthesis of Dimethyl Carbonate and Dimethoxymethane Over Cu-ZSM-5, *J. Catal.* **2006**, *244*, 219-229.

(15) Kaichev, V.V.; Popova, G.Ya.; Chesalov, Yu. A.; Saraev, A.A.; Zemlyanov, D.Y.; Beloshapkin, S.A.; Knop-Gericke, A.; Schlögl, R.; Andrushkevich, T.V.; Bukhtiyarov, V.I. Selective oxidation of Methanol to Form Dimethoxymethane and Methyl Formate Over a Monolayer V_2O_5/TiO_2 catalyst, *J. Cat.* **2014**, *311*, 59-70.

(16) Heqin, G.; Chen, C.; Yong, X.; Wang, J.; Fan, Z.; Li, D.; Sun, Y. Influence of Preparation Method on the Surface and Catalytic Properties of Sulfated Vanadia–Titania Catalysts for Partial Oxidation of Methanol, *Fuel Process. Tech.* **2013**, *106*, 77-83.

(17) El-Roz, M.; Lakiss, L.; Telegeiev, I.; Lebedev, O. I.; Bazin, P.; Vicente, A.; Fernandez, C.; Valtchev, V. High-Visible-Light Photoactivity of Plasma-Promoted Vanadium Clusters on Nanozeolites for Partial Photooxidation of Methanol, *ACS Appl. Mater. Interfaces* **2017**, *9*, 17846-17855.

(18) El-Roz, M.; Haidar, Z.; Lakiss, L.; Toufayli, J.; Thibault-Starzyk, F. Immobilization of TiO_2 Nanoparticles on Luffa Cylindrical Fibers for Photocatalytic Applications, *RCS Advances* **2013**, *3*, 3438-3445.

(19) El-Roz, M.; Lakiss, L.; Vicente, A.; Bozhilov, K. N.; Thibault-Starzyk, F.; Valtchev, V. Ultra-Fast Framework Stabilization of Ge-Rich Zeolites by Low-Temperature Plasma Treatment, *Chem. Sci.* **2014**, *5*, 68-80.

(20) El-Roz, M.; Lakiss, L.; El Fallah**,** J.; Lebedev**,** O. I.; Thibault-Starzyk**,** F.; Valtchev, V. Incorporation of Clusters of Titanium Oxide in Beta Zeolite Structure by a New Cold $TiCl_4$-Plasma Process: Physicochemical Properties and Photocatalytic Activity, *Chem. Phys. Phys. Chem.* **2013**, *38*, 16198-16207.

(21) Lakiss, L.; Rivallan, M.; Goupil, J.-M.; El Fallah, J.; Mintova, S. Self-Assembled Titanosilicate TS-1 Nanocrystals in Hierarchical Structures, *Catal. today* **2011**, *168*, 112-117.

(22)Thibault-Starzyk, F.; Gil, B.; Aiello, S.; Chevreau, T. ; Gilson, J.-P. In Situ Thermogravimetry in an Infrared Spectrometer: An Answer to Quantitative Spectroscopy of Adsorbed Species on Heterogeneous Catalysts, *Microporous Mesoporous Mater.* **2004**, *67*, 107-112.

(23) Wuttke, S.; Bazin, P.; Vimont, A.; Serre, C.; Seo, Y.-K.; Hwang, Y. K.; Chang, J.-S.; Férey, G.; Daturi, M. Discovering the Active Sites for C3 Separation in MIL-100(Fe) by Using Operando IR Spectroscopy, *Chem.-Eur. J.* **2012**, *18*, 11959-11967.

(24) El-Roz, M.; Monika, K.; Cool, P.; Thibault-Starzyk, F. New Operando-IR Technique to Study the Photocatalytic Activity and Selectivity of TiO_2… *J. Phys. Chem. C* **2012**, *116*, 13252-13263.

(25) El-Roz, M.; Bazin, P.; Thibault-Starzyk, F. An Operando-IR Study of Photocatalytic Reaction of Methanol on New *BEA Supported TiO_2 Catalyst, *Catal. Today* **2013**, *205*, 111-119.

(26) El-Roz, M.; Bazin, P.; Daturi, M.; Thibault-Starzyk, F. Operando Infrared (IR) Coupled to Steady-State Isotopic Transient Kinetic Analysis (SSITKA) for Photocatalysis: Reactivity and Mechanistic Studies, *ACS Catalysis*, **2013**, *3*, 2790-2798.

(27) El-Roz, M.; Bazin, P.; Daturi, M.; Thibault-Starzyk, F. On the Mechanism of Methanol Photooxidation to Methylformate and Carbon Dioxide on TiO_2: An Operando-FTIR Study, *Phys. Chem. Chem. Phys.* **2015**, *17*, 11277-11283.

(28) Zeng, D.; Liu, S.; Wang, G.; Chen, H.; Xu, J.; Deng, F. Effect of Surface Acid Properties of Modified VO_x/Al_2O_3 Catalysts on Methanol Selective Oxidation, *Catal. Lett.* **2013**, *143*, 624-629.

(29) Busca, G, Lamotte, J; Lavalley, J.-C.; Lorenzelli, V. FT-IR Study of the Adsorption and Transformation of Formaldehyde on Oxide Surfaces, *J. Am. Chem. Soc.*, **1987**, *109*, 5197-5202.

(30) Liu, Z.; Zhang, R.; Wang, S.; Li, N.; Sima, R.; Liu, G.; Wu, P.; Zeng, G.; Li, S.; Sun, Y. Highly Efficient and Stable Vanadia–Titania–Sulfate Catalysts for Methanol Oxidation to Methyl Formate: Synthesis and Mechanistic Study, *J. Phys. Chem. C*, **2016**, *120*, 659-6600.

(31) Li, N.; Wang, S.; Sun, Y.; Li, S. First Principles Studies on the Selectivity of Dimethoxymethane and Methyl Formate in Methanol Oxidation Over V_2O_5/TiO_2-Based Catalysts, *Phys. Chem. Chem. Phys.*, **2017**, *19*, 19393-19406.

(32) Kropp, T.; Paier, J.; Sauer, J. Support Effect in Oxide Catalysis: Methanol Oxidation on Vanadia/Ceria, *J. Am. Chem. Soc.* **2014**, *136*, 14616-14625.

(33) Zhao, G.; Yang, F.; Chen, Z.; Liu, Q.; Ji, Y.; Zhang, Y.; Niu, Z.; Mao, J.; Bao, X.; Hu, P.; Li, Y. Metal/Oxide Interfacial Effects on the Selective Oxidation of Primary Alcohols, *Nat. Commun.* **2017**, *8*, 1-8.

(34) Li, S.; Zheng, A.; Su, Y.; Zhang, H. ; Chen, L.; Yang, J.; Ye, Ch.; Deng, F. Brønsted/Lewis Acid Synergy in Dealuminated HY Zeolite: A Combined Solid-State NMR and Theoretical Calculation Study, *J. Am Chem. Soc.* **2007**, *129*, 11161-11171.

(35) Zheng, A.; Li, Sh.; Liu, Sh.; Deng, F. Acidic Properties and Structure–Activity Correlations of Solid Acid Catalysts Revealed by Solid-State NMR Spectroscopy, *Acc. Chem. Res.*, **2016**, *49*, 655–663.

(36) Wang, Ch.; Chu, Y.; Xu, J.; Wang, Q.; Qi, G.; Gao, P.; Zhou, X.; Deng, F. Extra-Framework Aluminum-Assisted Initial C–C Bond Formation in Methanol-to-Olefins Conversion on Zeolite H-ZSM-5, Angew. Chem. Int. Ed., **2018**, *57*, 10197-10201.

TOC